# Magnetotransport through graphene nanoribbons

Jeroen B. Oostinga,[1,2] Benjamin Sacépé,[1] Monica F. Craciun,[3] and Alberto F. Morpurgo[1]
[1]*DPMC and GAP, University of Geneva, 24 quai Ernest Ansermet, CH-1211 Geneva, Switzerland*
[2]*Kavli Institute of NanoScience, Delft University of Technology, P.O. Box 5046, 2600 GA Delft, The Netherlands*
[3]*Centre for Graphene Science, Department of Engineering, Mathematics and Physical Sciences, University of Exeter, North Park Road, Exeter EX4 4QF, United Kingdom*
(Received 20 April 2010; published 19 May 2010)

We investigate magnetotransport through graphene nanoribbons as a function of gate and bias voltage, and temperature. We find that a magnetic field systematically leads to an increase in the conductance on a scale of a few tesla. This phenomenon is accompanied by a decrease in the energy scales associated to charging effects, and to hopping processes probed by temperature-dependent measurements. All the observations can be interpreted consistently in terms of strong-localization effects caused by the large disorder present, and exclude that the insulating state observed in nanoribbons can be explained solely in terms of a true gap between valence and conduction bands.

DOI: 10.1103/PhysRevB.81.193408 PACS number(s): 85.35.−p, 72.80.Vp, 73.20.Fz, 73.23.−b

Single-layer graphene is a zero-gap semiconductor, whose valence and conduction bands touch at two inequivalent points (the K and K′ points) at the edge of the first Brillouin zone.[1] Owing to the absence of a band gap, the conductance of graphene remains finite irrespective of the position of the chemical potential. The impossibility to turn off the conductivity hinders the fabrication of high-quality field-effect transistors, and poses problems for the use of graphene in electronic devices. A possible solution is the use of graphene nanoribbons in which the opening of a gap between valence and conduction bands has been predicted theoretically.[2]

According to theory, a gap in nanoribbons should open as a consequence of size quantization and, depending on the specific case considered, interaction effects.[2] Transport experiments indeed find that the conductance through narrow ribbons is very strongly suppressed when the Fermi energy is close to the charge neutrality point.[3,4] However, it is unclear whether the opening of a band gap is the correct explanation for the experimental observations. On the one hand, a gap would lead to a conductance suppression similar to what is found experimentally, with characteristic energy scales (as probed in temperature- and bias-dependent measurements) comparable to the observed ones.[3] On the other hand, the theoretical predictions rely on edge structures that are ideal on the atomic scale whereas this is certainly not the case in real devices. This is why many theoretical studies have analyzed the role of strong localization of electron wave functions—possibly in combination with charging effects—as the origin of the conductance suppression observed in the experiments on nanoribbons.[5]

Existing studies of transport through graphene nanoribbons have mainly relied on measurements of conductance as a function of carrier density and temperature, and have not led to a definite conclusion as to the nature of the transport gap. Here, we present a systematic investigation focusing on the magnetotransport properties. We show that, in the transport gap, the application of magnetic field always leads to a conductance increase, together with a decrease in the characteristic energy scale associated to the conductance suppression. We perform an analysis of these measurements that excludes the opening of a band gap as the sole explanation for the observed insulating behavior, and accounts for all our observations (including the gate-voltage and temperature dependence) in a consistent way, in terms of strong-localization effects caused by the larger disorder present in narrow ribbon geometries.

We have investigated many devices consisting of graphene nanoribbons fabricated using the by-now conventional exfoliation procedure. The details of the device fabrication process and ribbon patterning (based on etching in an Ar plasma) are identical to those that we have used for the realization of Aharonov-Bohm rings (see Ref. 6). The device geometry is schematically shown in the inset of Fig. 1(a). Different dimensions were used, with the ribbon width $W$ varying approximately between 50 and 100 nm, and the ribbon length $L$ between 500 and 1000 nm. The region where the metal electrodes contact the graphene layer is intentionally kept large to exclude effects due to the contact resistance. Conductance measurements on many different devices yielding consistent results were performed in a two-terminal configuration as a function of backgate voltage, temperature, and magnetic field. Unless stated otherwise, here we show data obtained from one of these ribbons (with length $L$

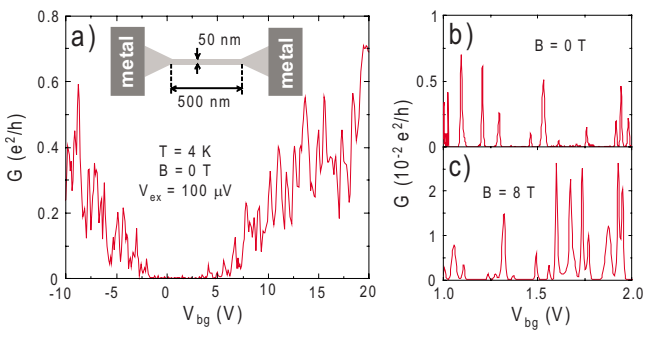


FIG. 1. (Color online) (a) Conductance $G$ as a function of the gate voltage $V_{bg}$, showing a transport gap at low charge densities. The inset shows a scheme of the device geometry (the substrate is highly doped silicon covered by a 285 nm $SiO_2$ layer). Panels (b) and (c) zoom in on the Coulomb-blockade peaks present in the transport gap at $B=0$ T and 8 T, respectively.

 

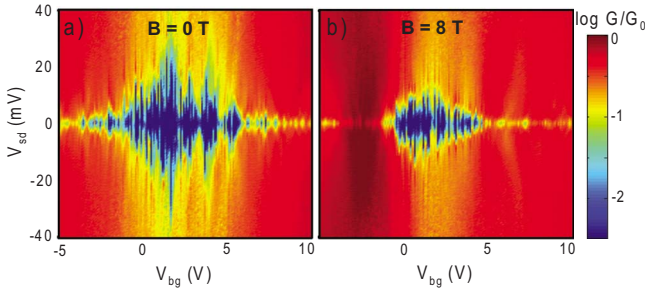


FIG. 2. (Color online) Panels (a) and (b) show the color plots of $\log(G)$ as a function of gate ($V_{bg}$) and bias ($V_{sd}$), respectively, at $B=0$ and 8 T (the measurements are taken at $T=4.2$ K; $G_0=e^2/h$). The comparison of the two panels shows how in a magnetic field the extent of the high-resistance part is suppressed.

$=500$ nm and width $W=50$ nm), representative of the overall behavior observed.

Figure 1(a) shows the linear conductance $G$ of the ribbon as a function of gate voltage. The conductance is strongly suppressed in the voltage range $[-2\ \text{V}, +4\ \text{V}]$, that we refer to as the transport gap (the transport gap depends weakly on the ribbon length and it is larger for longer devices, consistently with the results of Ref. 7). Figure 1(b) zooms in on this range, showing conductance peaks at several gate voltages (with the conductance vanishing elsewhere) originating from charging effects. Measurements as a function of gate ($V_{bg}$) and bias ($V_{sd}$) voltage show that the conductance is highly suppressed at low $V_{sd}$ [Fig. 2(a)], and exhibit characteristic "diamondlike" structures [Fig. 3(a)] typical of Coulomb blockade. These results are similar to others already reported,[3,4] and clearly indicate that the electrons are confined in small regions of the ribbon—which we call islands—whose area is sufficiently small to have a significant charging energy. Figure 3(a) shows that the diamonds are irregular and partially overlap, indicating that the islands in the ribbon vary in size and that electrons have to propagate through several of them while traversing the ribbon. At a microscopic level, the question is what is the mechanism that determines the presence of the islands, i.e., the presence of a band gap or the effect of strong localization.

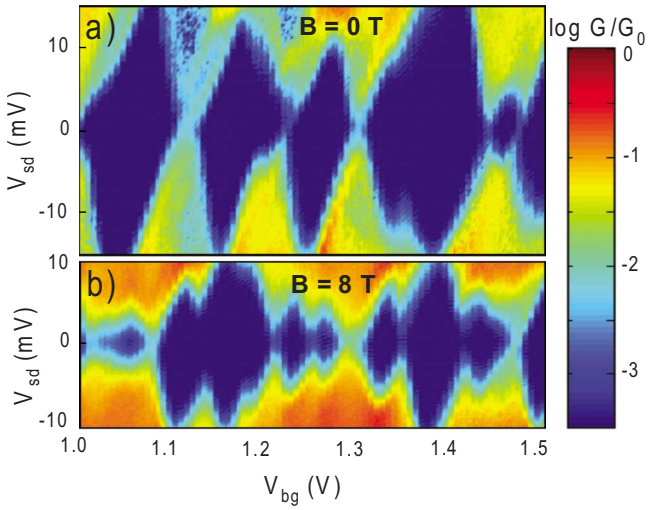


FIG. 3. (Color online) Coulomb diamonds measured in the transport gap at $T=4.2$ K, at (a) $B=0$ T and (b) $B=8$ T. The typical height $\Delta V_{sd}$ and width $\Delta V_{bg}$ of the diamonds at high field are smaller than at zero field.

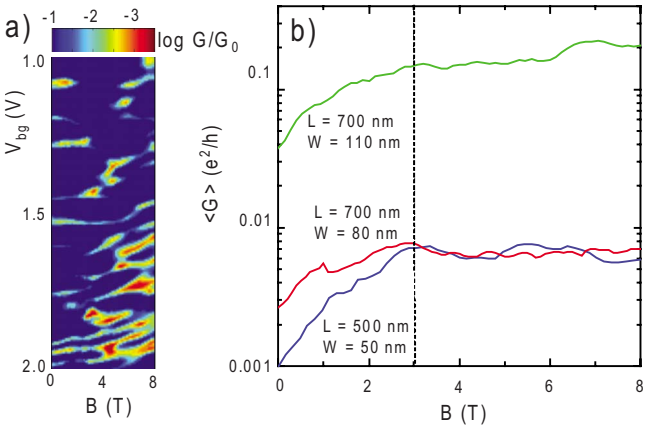


FIG. 4. (Color online) (a) Color plot of $\log(G)$ as a function of $V_{bg}$ (in the transport gap) and of $B$ (measurements done at $T=4.2$ K). The average peak conductance and the number of Coulomb peaks increase with increasing magnetic field [consistent with Figs. 1(b) and 1(c) and Fig. 3]. Panel (b) shows the average of conductance over gate voltage, as a function of magnetic field. Noticeably, this quantity increases with increasing $B$ up to approximately 3 T (irrespective of the ribbon width), and saturates for higher-field values.

The analysis of the influence of magnetic field provides additional important information. In Figs. 2(a) and 2(b), the conductance measured as a function of gate and bias voltage at $B=0$ and 8 T can be directly compared. The bias and gate-voltage ranges where the conductance is suppressed are significantly smaller when a high magnetic field is applied. Also the Coulomb peaks and diamonds are affected [compare Figs. 1(b) and 1(c) and Figs. 3(a) and 3(b)]: in the presence of a high magnetic field, the average number of Coulomb peaks in a given gate-voltage range is larger, and the average peak conductance is higher. Qualitatively, these observations indicate that the average island size increases when a magnetic field is applied since for larger islands, the charging energy is smaller.

The continuous evolution from $B=0$ to 8 T is shown in Fig. 4(a). In Fig. 4(b), we show the average (over gate voltage varying in the transport gap) of the conductance as a function of magnetic field. Since the conductance between the Coulomb peaks is negligibly small, this quantity measures the average peak conductance and the number of peaks present. Figure 4(b) shows the average conductance for the sample that we are discussing, and for two other nanoribbons having width $W=80$ nm and $W=110$ nm. We see that the average conductance increases with magnetic field for $B<3$ T and that it saturates for $B>3$ T. We conclude that the average number of Coulomb peaks and the peak conductance increase for $B<3$ T but remains approximately constant for $B>3$ T. Unexpectedly, the average conductance saturates at approximately similar values of the magnetic field in the different devices, irrespective of the ribbon width.

In order to analyze the results of the magnetotransport

experiments, we first go back to the data shown in Fig. 1(a), and look at a larger gate-voltage range (outside the transport gap), to estimate the value of the electron mean-free path. From the average slope (i.e., neglecting the fluctuations) of the conductance versus gate voltage, $\partial G/\partial V_{bg}$, measured at high charge density (where the conductance is much larger than in the transport gap), we determine the field-effect mobility $\mu_{FET}=\frac{tL}{W\epsilon_r\epsilon_0}\frac{\partial G}{\partial V_{bg}}\approx 1000$ cm$^2$/V s. This value is smaller than the typical values usually found for large graphene flakes on $SiO_2$ substrates ($\mu\sim 5000-10\,000$ cm$^2$/V s),[1] confirming that graphene nanoribbons are more disordered.[8] We determine $l_m$ using the Einstein relation $\sigma=\nu e^2 D$, where $D$ is the diffusion constant and $\nu$ the density of states $[\nu(\varepsilon_F)=8\pi|\varepsilon_F|/(h^2v_F^2)]$, with $\varepsilon_F$ and $v_F$ the Fermi energy and velocity, respectively. From the conductivity, $\sigma\approx G_{square}=GL/W$ measured at $V_{bg}=-10$ V, and determining $\varepsilon_F$ from the charge-density-induced electrostatically $n(V_{bg}=-10\text{ V})=4\pi\varepsilon_F^2/(h^2v_F^2)\approx 1\times 10^{12}$ cm$^{-2}$, we obtain $D\approx 0.006$ m$^2$/s. The corresponding electron mean-free path is then obtained from $l_m=2D/v_F\approx 10$ nm, smaller than the ribbon width ($W=50$ nm).

The short mean-free path values are indicative of strong disorder, and suggest that a scenario based on strong localization may be appropriate (consistently with the conclusion reported recently in Ref. 7, and theoretical predictions[5]). A signature of strong localization is a positive magnetoconductance, originating from an increase in the localization length due to time-reversal symmetry breaking.[9,10] In the strong-localization regime, time-reversal symmetry is broken when the magnetic flux through an area corresponding to the square of the localization length $\xi^2$ is on the order of the flux quantum $h/e$. This mechanism can explain our data of Fig. 4(b), which show that the average conductance at low $n$ does indeed increase when the magnetic field is increased from 0 to $\sim 3$ T, and provide an estimate of the localization length of $\xi\approx(h/eB)^{1/2}\approx 35-40$ nm. This value of $\xi$ is somewhat smaller than (but comparable with) the width of the three ribbons whose data are plotted in Fig. 4(b): this is why the magnetoconductance saturates at approximately the same magnetic field in the different devices. Further, we estimate the phase coherence length $l_\varphi=(D\tau_\varphi)^{1/2}$ by using the value of the diffusion constant obtained above and the phase coherence time $\tau_\varphi\approx 5$ ps reported in Ref. 11. We obtain $l_\varphi\approx 175$ nm, from which we conclude that $l_m<\xi<l_\varphi$, the correct hierarchy of length scales for the strong-localization regime.[9] Note also that at low charge density, where the number of transverse channels occupied is small and $\xi\sim l_m$, as expected from theory.[9] The increase in conductance observed at higher charge density can then be attributed to an increase in localization length, due to the increase in the number of occupied transverse channels.

It is particularly important to discuss whether the observed positive magnetoconductance can be understood if the formation of islands in the ribbons is due to the opening of a band gap (and not by strong-localization effects). In the presence of a high magnetic field, well-defined Landau levels are expected to appear in the energy spectrum when the magnetic length, $l_B=(\hbar/eB)^{1/2}$ becomes sufficiently smaller than the ribbon width (when $l_B\ll W$, the finite width does not affect the Landau levels). Owing to the presence of a zero-energy Landau level in graphene,[12] a large magnetic field should cause the closing of the gap and lead to the appearance of edge states that would contribute to the conductance ($\sim e^2/h$). This mechanism could explain a positive magnetoconductance. In the experiments, however, we do not observe any signature of the formation of edge states—the low-temperature conductance in the transport gap remains always much smaller than $e^2/h$—despite the fact that $l_B\approx 10$ nm for $B=8$ T (ten times smaller than the largest ribbon that we discuss here). This observation again implies that ribbons are highly disordered even for the widest ribbon disorder is strong enough to cause backscattering between counter-propagating states at opposite edges, leading to their localization. In other words, even if we attempt to explain the positive magnetoconductance in terms of a band gap, we are forced to conclude that localization effects are nevertheless dominating.[13]

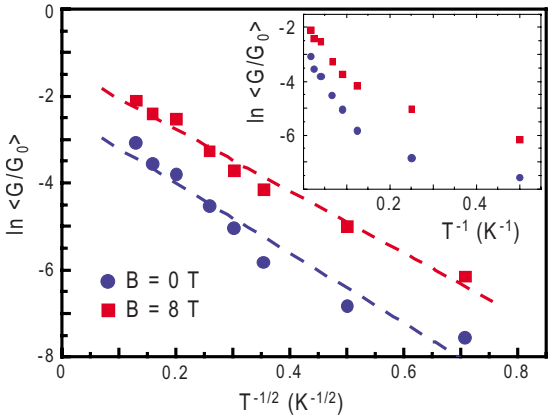


FIG. 5. (Color online) The average conductance $\langle G\rangle$ in the transport gap as a function of $T^{-1/2}$ at $B=0$ T and $B=8$ T. The dashed lines are linear fits to the data. In the inset, the same data is plotted as a function of $T^{-1}$.

We now look at the temperature dependence of the conductance measured in the transport gap. For strongly localized electrons, transport occurs via either nearest-neighbor hopping (NNH) or variable-range hopping (VRH),[9] and the latter mechanism dominates at low temperature. Figure 5 shows the measurement of the gate-averaged conductance in the transport gap as a function of temperature in the range 2–60 K, for $B=0$ T and $B=8$ T. In case of NNH, the temperature dependence of the conductance should be proportional to $G\propto\exp-(T_0/T)$. However, the plot shown in the inset of Fig. 5 indicates that Arrhenius law does not reproduce the data well. Rather, the data fits better to $G\propto\exp-(T_0/T)^{1/2}$, which is the temperature dependence expected for VRH (see Fig. 5). The exponent $n=1/2$ corresponds to two-dimensional hopping in the presence of Coulomb interaction (which is expected given the obvious presence of Coulomb-blockade effects) or for quasi-one-dimensional hopping with or without interactions. This behavior indicates that electronic transport is dominated by variable-range hopping.

The parameter $T_0$ is related to the energy needed by an electron to hop between localized states. From the linear fit to the data of Fig. 5, we obtain $kT_0\approx 6$ meV at $B=0$ T and

a smaller value, $kT_0 \approx 4$ meV at $B=8$ T when time-reversal symmetry is broken. This result agrees with what we would expect if $\xi$ is larger at high magnetic field. Indeed, the relevant energy scales of the localized states involved in the hopping are the single-particle level spacing and the charging energy, which are inversely proportional to the extension of the wave function of the localized states (i.e., they decrease when $\xi$ increases). The values found for $T_0$ are, as expected for the variable-range-hopping regime, a fraction of the characteristic values of single level spacing and charging energy, which, depending on the detail of the estimate range from about 10 meV to a few tens of millielectron volt (at $B=0$ T, with $\xi \simeq 35-40$ nm).

In summary, magnetotransport experiments provide a consistent picture as to the origin of the transport gap observed in graphene nanoribbons: they indicate that strong-localization effects—and not a gap between valence and conductance bands—are the cause of the observed insulating state that is observed experimentally.

We thank Y. Blanter, L. Vandersypen, and M. Fogler for useful discussions, and S. Russo for support in fabricating several devices. This work was supported by the NWO VICI, NanoNed, the Swiss National Science Foundation (Project No. 200021-121569), and by the NCCR MaNEP.

[1] A. K. Geim and K. S. Novoselov, Nat. Mater. **6**, 183 (2007).

[2] K. Nakada, M. Fujita, G. Dresselhaus, and M. S. Dresselhaus, Phys. Rev. B **54**, 17954 (1996); Y.-W. Son, M. L. Cohen, and S. G. Louie, Phys. Rev. Lett. **97**, 216803 (2006); L. Brey and H. A. Fertig, Phys. Rev. B **73**, 235411 (2006).

[3] M. Y. Han, B. Özyilmaz, Y. Zhang, and P. Kim, Phys. Rev. Lett. **98**, 206805 (2007).

[4] Z. Chen *et al.*, Physica E **40**, 228 (2007); K. Todd *et al.*, Nano Lett. **9**, 416 (2009); C. Stampfer, J. Güttinger, S. Hellmüller, F. Molitor, K. Ensslin, and T. Ihn, Phys. Rev. Lett. **102**, 056403 (2009); X. Liu, J. B. Oostinga, A. F. Morpurgo, and L. M. K. Vandersypen, Phys. Rev. B **80**, 121407(R) (2009); P. Gallagher, K. Todd, and D. Goldhaber-Gordon, *ibid.* **81**, 115409 (2010).

[5] F. Sols, F. Guinea, and A. H. Castro Neto, Phys. Rev. Lett. **99**, 166803 (2007); D. Gunlycke, D. A. Areshkin, and C. T. White, Appl. Phys. Lett. **90**, 142104 (2007); A. Lherbier, B. Biel, Y.-M. Niquet, and S. Roche, Phys. Rev. Lett. **100**, 036803 (2008); M. Evaldsson, I. V. Zozoulenko, H. Xu, and T. Heinzel, Phys. Rev. B **78**, 161407(R) (2008); E. R. Mucciolo, A. H. Castro Neto, and C. H. Lewenkopf, *ibid.* **79**, 075407 (2009); I. Martin and Y. M. Blanter, *ibid.* **79**, 235132 (2009).

[6] S. Russo, J. B. Oostinga, D. Wehenkel, H. B. Heersche, S. S. Sobhani, L. M. K. Vandersypen, and A. F. Morpurgo, Phys. Rev. B **77**, 085413 (2008).

[7] M. Y. Han, J. C. Brant, and P. Kim, Phys. Rev. Lett. **104**, 056801 (2010).

[8] The enhanced disorder in nanoribbons probably orginates from a combination of intervalley scattering due to atomic-scale edge roughness, and larger potential fluctuations due to chemical species saturating the dangling bonds at the edges.

[9] B. I. Shklovskii and A. L. Efros, *Electronic Properties of Doped Semiconductors* (Springer, Heidelberg, Germany, 1984); Y. Imry, *Introduction to Mesoscopic Physics* (Oxford University Press, Oxford, UK, 1997); Y. V. Nazarov and Y. M. Blanter, *Quantum Transport: Introduction to Nanoscience* (Cambridge University Press, Cambridge, UK, 2009).

[10] M. E. Gershenson, Y. B. Khavin, A. G. Mikhalchuk, H. M. Bozler, and A. L. Bogdanov, Phys. Rev. Lett. **79**, 725 (1997).

[11] F. V. Tikhonenko, D. W. Horsell, R. V. Gorbachev, and A. K. Savchenko, Phys. Rev. Lett. **100**, 056802 (2008).

[12] K. S. Novoselov *et al.*, Nature (London) **438**, 197 (2005); Y. Zhang *et al.*, *ibid.* **438**, 201 (2005).

[13] At 8 T, the energy gap between the lowest Landau levels is much larger than the expected band gap since features associated to Landau levels are not visible, the much smaller band gap should also not be expected to determine the device properties.